International Journal of Geospatial and Environmental Research

Volume 11 | Number 1 Article 1

February 2024

The Usage of Band Ratios to Predict Lake Water Quality Parameters using Sentinel-2 L1C Imagery

Austin Spoor
University of Nebraska-Lincoln, aspoor2@huskers.unl.edu

Ho-Seop Cha
Park University, hoseop.cha@park.edu

Recommended Citation
Spoor, Austin and Cha, Ho-Seop (2024) "The Usage of Band Ratios to Predict Lake Water Quality Parameters using Sentinel-2 L1C Imagery," *International Journal of Geospatial and Environmental Research*: Vol. 11: No. 1, Article 1.
Available at: https://dc.uwm.edu/ijger/vol11/iss1/1

The Usage of Band Ratios to Predict Lake Water Quality Parameters using Sentinel-2 L1C Imagery

Abstract

Band ratios using remote imagery can be useful for monitoring large bodies of water when high quality imagery is available. Sentinel-2 satellite imagery provides frequent, high-resolution coverage of the globe. This study set out to test the usefulness of existing band ratios for estimating chlorophyll a (CHL-*a*), dissolved organic carbon (DOC), and turbidity with Sentinel-2 imagery. USGS in-situ data was matched to Sentinel-2 imagery of Beaver Lake, Arkansas taken August 2015 to July 2019 and the dark spectrum fitting (DSF) atmospheric correction method in ACOLITE was applied to generate surface reflectance values. CHL-*a* was estimated using two different methods, the band 5 (B5) peak at 704.1 nm and the ratio of B5 to B4. DOC was estimated using the ratio of B3 to B4. A turbidity estimation equation was created by directly correlating turbidity to B4 reflectance values. The usage of these methods was deemed to be unfit for use under the conditions found at Beaver Lake. Poor correlation was found for CHL-*a* ($R^2 = 0.0228$, $R = -0.1510$, & $R^2 = 0.0344$, $R = 0.1855$) and for DOC ($R^2 = 0.0548$, $R = -0.2341$). Turbidity was more strongly corelated to the estimate equation ($R^2 = 0.8402$, $R = 0.9166$) but considering the poor results for other parameters it is not recommended to apply these methodologies to parameter estimation at Beaver Lake.

Keywords

Remote Sensing, Water Quality, chlorophyll a (CHL-a), dissolved organic carbon (DOC), Turbidity

1. Introduction

Remote imagery of the earth's surface is gathered continuously by a global network of satellites such as the European Space Agency's Sentinel-2 mission which launched in June 2015 [12]. The Sentinel-2 mission is designed for vegetation monitoring but valuable for the remote water monitoring community [2, 29]. The mission makes this data freely available like other pre-existing land-focused systems such as the U.S. Geological Survey's (USGS) Landsat Program [15]. The Sentinel-2 mission is composed of 2 satellites, Sentinel-2A and Sentinel-2B carrying a Multi Spectral Instrument (MSI) which captures imagery in 13 bands [7]. These satellites produce images in a 290 km swath, with each spectral band having a spatial resolution of 10-60 m dependent upon the spectral band (Table 1). Combining imagery from both satellites in the mission gives an equatorial temporal resolution of 5 days [12]. These bands range from 442-2202 µm, covering part of the visible and infrared spectrums [20]. B1 measuring reflectance at 442 µm and B12 measuring reflectance values at 2202 µm (Table 1).

Sentinel-2 imagery has been studied in the literature for its usage in remote water monitoring [13]. Using remote imagery is a useful substitute for the more expensive and time-consuming method of in-situ monitoring [22]. Successful utilization of remote sensing techniques for water quality monitoring can increase the spatial and temporal resolution of water quality data, which is why band ratios have been utilized in Europe to meet the European Union's reporting requirements for monitoring lakes [5]. As band ratios are deemed to be useful equipment in the monitoring process for large bodies of water with high quality imagery like Sentinel-2, this paper attempts to examine how useful existing band ratios are when utilized to estimate chlorophyll a (CHL-*a*), dissolved organic carbon (DOC), and turbidity with Sentinel-2 imagery. Freshwater lake water quality is important as lakes provide water and recreation sources to many people and Sentinel-2 offers both good spatial and temporal resolution [19]. This resolution makes frequently monitoring large areas more economically viable and timely than in-situ testing and lab work.

2. Materials and Methods

2.1. Study Site and Data

Beaver Dam and Lake were constructed from 1960-1966 [31]. The dam was built across the White River in Northwestern Arkansas, USA [24]. The surrounding area has since urbanized significantly, highlighting the importance of water quality monitoring. The lake is used for hydroelectric power generation, as a reservoir for drinking water and for recreational boating and swimming. The lake surface totals 114 km^2 with an average depth of 18.3 m and a maximum depth of 73 m [31]. The dam is located at USGS sample point 07049500 as seen in Figure 1.

USGS Arkansas Water Science Center collected in-situ samples as indicated in

Table 1. All samples were tested at the USGS-National Water Quality Lab (NWQL) in Denver, Colorado. CHL-*a* data were collected in μg/L according to Environmental Protection Agency (EPA) Method 445.0 [3]. USGS-NWQL Rapi-Note 17-22 [32] was used to record DOC in mg/L. Turbidity data were collected in Nephelometric Turbidity Ratio Unit (NTRU) according to EPA method 180.1 [9]. All in-situ USGS data were downloaded from The Water Quality Portal [30] for the four sample sites.

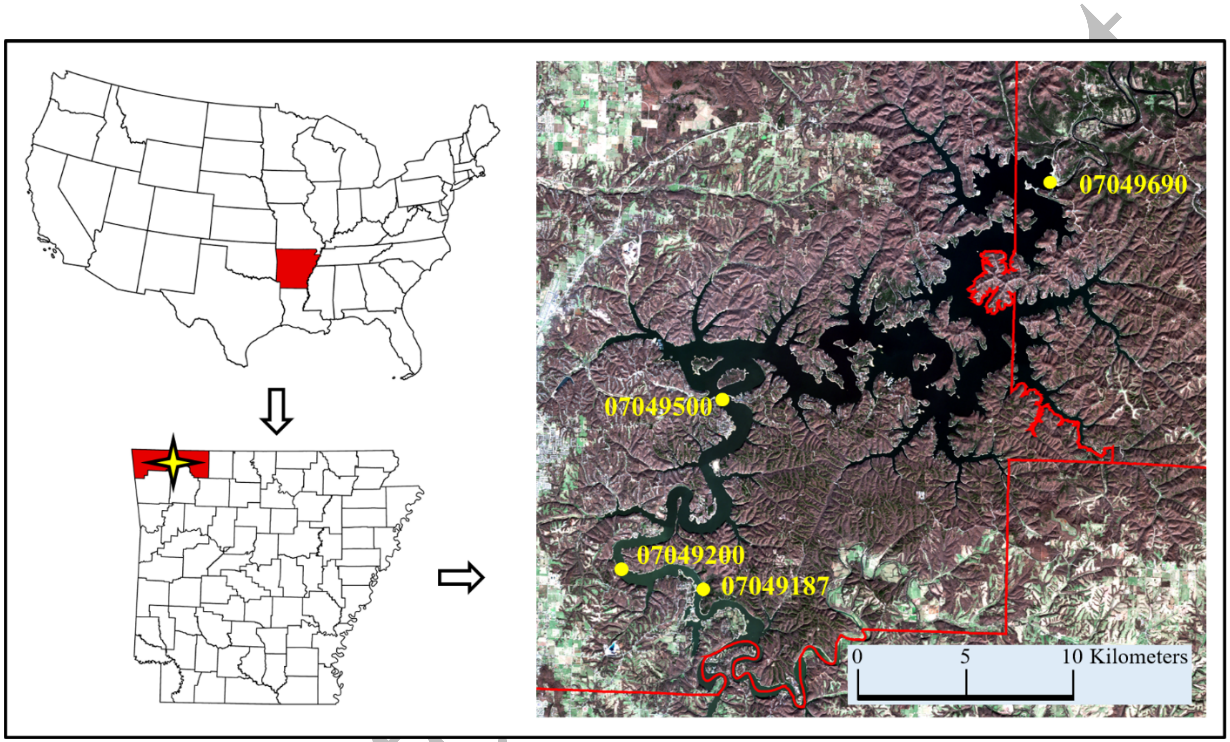

Figure 1 The location of Beaver Lake, Arkansas within the United States and a Sentinel-2 image of the study area within Northwest Arkansas overlaid with counties and sample sites. Three of the USGS sample sites are located in Benton County, 07049500, 07049200, and 07049187. One site is located in Carrol County, 07049690.

2.2. Sentinel-2 Data

In-situ data collected on 22 dates from August 6, 2015 to July 11, 2019 were chosen for comparison by searching on the European Space Agency's Copernicus Open Access Hub [10] for available Sentinel-2 imagery. Only images with less than 30% cloud coverage and taken ±4 days [17] of available in-situ data were selected for usage. Fourteen images matched with the 22 sample dates and met these criteria (Table 1). The average time between an image and the corresponding in-situ measurement was 1.5 days. The Sentinel-2 imagery was retrieved as a Level-1C (L1C) product. Sentinel-2 L1C imagery are 100 × 100 km square orthorectified tiles of each band in UTM/WGS84 projection [11].

Each tile contains Top of Atmosphere (TOA) reflectance values and spatial resolution varies by band (Table 1). ACOLITE [28] is an atmospheric correction software used for remote imagery analysis. ACOLITE version 20190326.0 on Windows 10 (64 bit) was used to subset and resample the L1C products to a consistent 20 m resolution [26] (see Note 1). The dark spectrum fitting (DSF) atmospheric correction method found in ACOLITE [27] was applied for atmospheric correction, to obtain Bottom of Atmosphere (BOA) reflectance value. After subset, resampling, and atmospheric correction (see Note 2), MultiSpec [4] version 2018.08.30 on Windows 10 (64 bit) was used to generate each band's 9 pixel-value mean from a histogram summary of a 3 x 3 grid at each of the four sample points (Figure 1) for both TOA and BOA reflectance values.

Image Date (mm/dd/yyyy)	Site	In-situ Date	CHL-*a* (µg/L)	DOC (mg/L)	Turbidity (NTRU)
8/6/2015	07049187	8/6/2015	6.0	2.78	3.6
8/6/2015	07049200	8/6/2015	5.80	2.65	2.8
8/6/2015	07049500	8/6/2015	4.2	2.64	7.4
8/16/2015	07049690	8/18/2015	1.6	2.36	2.3
11/14/2015	07049187	11/10/2015	5.5	2.37	6.5
4/2/2016	07049187	3/31/2016	6.9	1.54	11
7/21/2017	07049187	7/18/2017	3.3	3.23	2.1
7/21/2017	07049200	7/19/2017	4.00	3.16	2.0
7/21/2017	07049500	7/18/2017	2.4	3.16	10
7/21/2017	07049690	7/18/2017	0.8	1.97	2.0
11/23/2017	07049187	11/21/2017	4.2	2.14	7.0
12/13/2017	07049187	12/13/2017	4.3	2.16	4.8
12/13/2017	07049200	12/13/2017	2.80	2.16	4.5
12/13/2017	07049500	12/14/2017	4.1	2.2	4.2
12/13/2017	07049690	12/14/2017	1.5	2.0	NA
3/13/2018	07049187	3/13/2018	2.3	2.48	40
3/13/2018	07049500	3/12/2018	4.7	2.41	32
3/13/2018	07049690	3/12/2018	1.4	1.91	2.0
4/27/2018	07049187	4/24/2018	5.2	2.38	18
5/22/2018	07049187	5/22/2018	6.4	3.15	13
5/22/2018	07049500	5/23/2018	7.9	2.45	3.4
5/22/2018	07049690	5/23/2018	0.6	2.1	NA
7/21/2018	07049187	7/18/2018	10.40	2.47	NA
7/21/2018	07049200	7/18/2018	13	NA	2.0
7/21/2018	07049500	7/19/2018	8.5	2.1	5.5
7/21/2018	07049690	7/19/2018	1.0	2.04	4.4
9/19/2018	07049187	9/18/2018	4.40	2.23	NA
9/19/2018	07049200	9/18/2018	5.5	2.27	NA
9/19/2018	07049500	9/19/2018	3.1	2.38	2.0
9/19/2018	07049690	9/19/2018	1.30	2.25	2.2
1/27/2019	07049200	1/30/2019	1.1	1.94	18
1/27/2019	07049500	1/30/2019	3.9	1.94	9.1
1/27/2019	07049690	1/31/2019	2.20	2.02	2.0
7/11/2019	07049200	7/10/2019	6.8	2.41	2.4
7/11/2019	07049500	7/11/2019	4.2	2.4	32

7/11/2019	07049690	7/10/2019	0.9	1.8	NA

Table 1 In-situ data collected by USGS at Beaver Lake, Arkansas and, the corresponding Sentinel-2 imaging dates matched to the data. No data collected is indicated by NA.

2.3. Band Ratios

Band ratios and remote sensing algorithms have been developed for use with the large variety of available spaceborne and aerial imaging sensors [13]. Considering the available in-situ parameters and algorithms in the literature, CHL-*a*, DOC, and Turbidity were determined to be the most suitable parameters and 4 algorithms were chosen to estimate these parameters. CHL-*a* is an important and well-studied parameter which can indicate general lake quality and therefore had 2 different band ratios used for estimation [13].

CHL-*a* has been known to reflect light most strongly near 700μm since at least 1992 [14]. B5 on Sentinel-2's MSI has a peak at 704.1 μm (Table 1), making it the closest band to estimate CHL-*a*. The average of the surrounding bands of B4 and B6 was removed from the reflectance value of B5 to narrow focus on the central band producing a parameter estimate of (B5 – ((B4 + B6)/2)) [26]. This estimate was applied for CHL-*a* and also used for DOC [26]. CHL-*a* has also been found to be linearly correlated with the ratio of ((705 μm)/(675 μm)) [23] which would be most closely applied to Sentinel-2 analysis by the parameter estimate of (B5/B4).

In-situ turbidity measurements have been found to correlate strongly to the reflectance values of B3 of Landsat 7 ETM+ [21]. This red band [8] correlates to B4 on the Sentinel-2 MSI. B4's reflectance values were used to linearly correlate in-situ turbidity. Colored Dissolved Organic Matter (CDOM) and DOC can be estimated using the same band math [33]. CDOM data was unavailable for the sites, but DOC was available, therefore the CDOM estimate of (B3/B4) was used to estimate DOC [26].

3. Results and Discussion

Both water quality monitoring data and useable satellite imagery were available for the years 2015 through 2019 (Table 2). Every month except June and October had at least one dataset available for use, providing a study covering seasonal variation over 4 years. In-situ CHL-*a* levels were measured in the range of 0.6 - 13 μg L^{-1}, DOC from 1.54 - 3.23 mg L^{-1} with only 1 site missing an in-situ value, and turbidity from 2 - 40 NTRU with 6 sites missing an in-situ value for a Sentinel-2 product (Table 2). The 3 x 3 averaged reflectance values were used as input for all band ratios.

Microsoft Excel was used to calculate band ratio values, utilizing the MultiSpec output of reflectance values per band. Band ratio values were correlated with available in-situ data (Figures 2-5). The Pearson correlation coefficient (R) values were calculated for each pairing and are presented in Table 3.

The R values for CHL-*a* and (B5 – ((B4 + B6)/2)) were -0.1192 and -0.1510 respectively for BOA and TOA. The R values for CHL-*a* and (B5/B4) were found to be 0.1208 and 0.1855 respectively for BOA and TOA. These R values for CHL-*a* were the only R values where TOA reflectance values had a stronger correlation to in-situ data than BOA reflectance values had. R values for DOC and (B3/B4) were -0.2238 and -0.2341 respectively for BOA and TOA. The R values for Turbidity and B4 were the strongest at 0.9166 and 0.8736 for BOA and TOA respectively. These results generally show a poor correlation between the in-situ data and the band ratios used for the atmospherically corrected products.

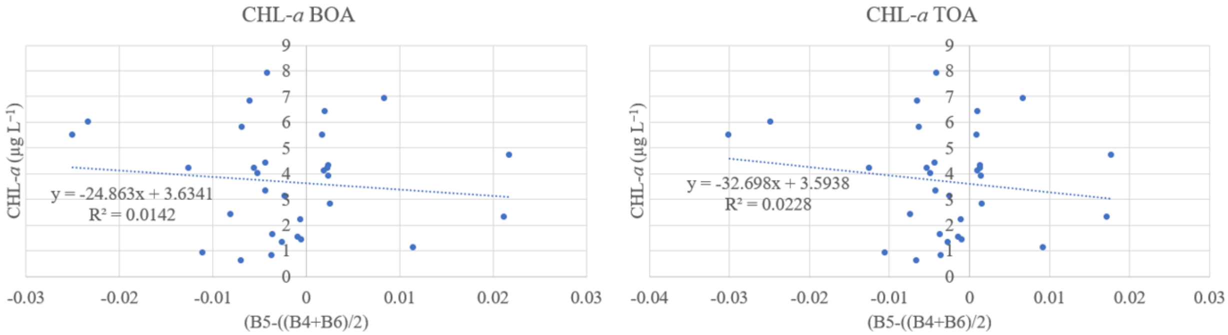

Figure 2 Represents correlation of the reflectance peak of B5 from L1C products to in-situ CHL-a data for both the atmospherically corrected BOA reflectance on the left and the uncorrected TOA reflectance on the right.

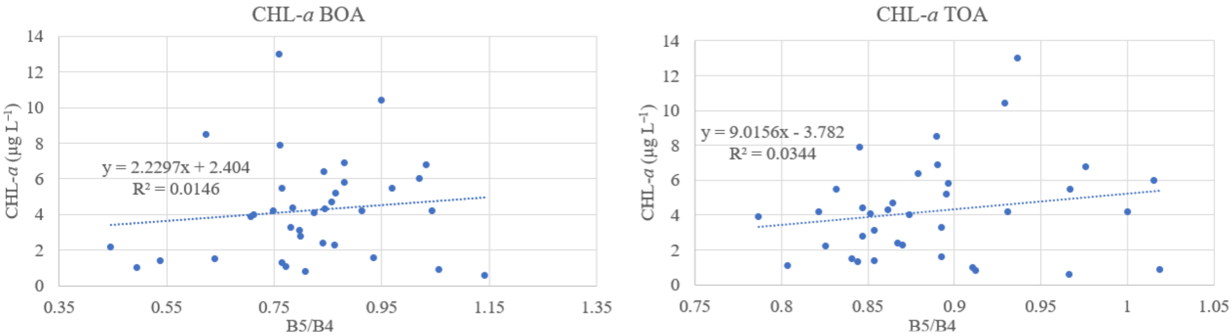

Figure 3 Represents correlation of the ratio of B5 to B4 from L1C products to in-situ CHL-a data for both the atmospherically corrected BOA reflectance on the left and the uncorrected TOA reflectance on the right.

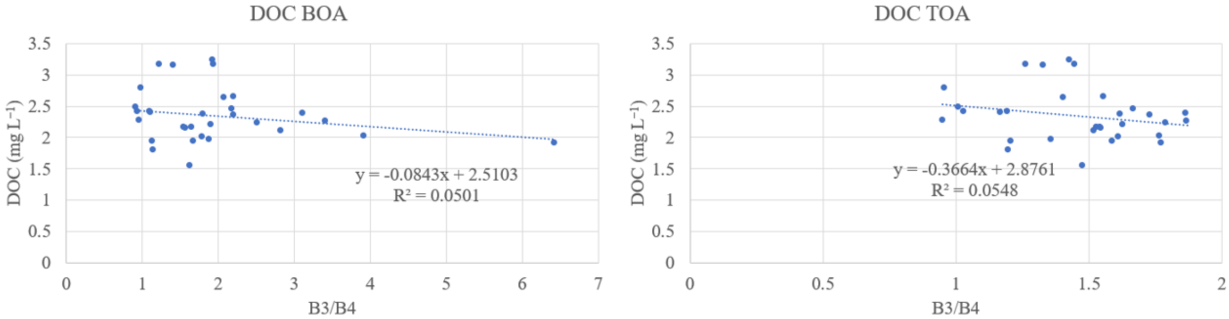

Figure 4 Represents correlation of the ratio of B3 to B4 from L1C products to in-situ DOC data for both the atmospherically corrected BOA reflectance on the left and the uncorrected TOA reflectance on the right.

In-situ Value & Band Ratio	R
In-situ CHL-*a* & BOA (B5-((B4+B6)/2))	-0.1192
In-situ CHL-*a* & TOA (B5-((B4+B6)/2))	-0.1510
In-situ CHL-*a* & BOA B5/B4	0.1208
In-situ CHL-*a* & TOA B5/B4	0.1855
In-situ DOC & BOA B3/B4	-0.2238
In-situ DOC & TOA B3/B4	-0.2341
In-situ Turbidity & BOA B4	0.9166
In-situ Turbidity & TOA B4	0.8736

Table 2 A comparison of in-situ values measured and band ratio investigated along with the Pearson correlation coefficient (R)

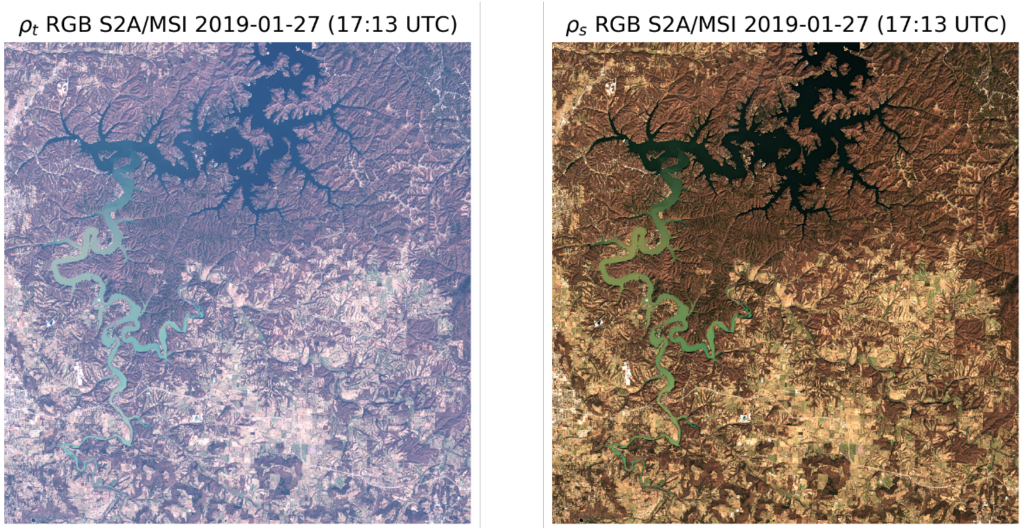

Figure 5 ACOLITE's atmospherically uncorrected TOA (ρ_t, left) and corrected BOA (ρ_s, right) natural color band combination (RGB B4, B3, B2) of the Sentinel-2A L1C MSI product for the Beaver Lake, Arkansas area on January 27, 2019.

AOLITE's implementation of DSF has specifically been tested as an improvement to existing methods for atmospheric correction over water bodies [27, 29]. The resulting imagery had a noticeable decrease in atmospheric interference after correction (see Figure 6). In the best of cases, the very clear imagery found in Figure 6 was produced. However, the Southern portion of Beaver Lake had particularly frequent issues with poor correction (see Figure 7). It is unfair to blame DSF or ACOLITE for the poor outcomes as they performed well under appropriate circumstances. The most common issue was the frequent cloud cover over the study area.

The band ratios used were successful for the authors who presented their usage, but they were largely unhelpful in the study of Beaver Lake. Possible reasons for this failure are the usage of all-season data for developing the correlating equations. There are many variables which impact the precise relationship between in-situ data and any successful correlation, which is the reason a unique equation must be developed for every site and no universal equations exist. Each site must have its own coefficients for the models to work at the given locale. Simple linear models for water quality parameters have shown success in the literature [1,13,18,26] but in some locales, a more complicated model is necessary to achieve high correlations [6,16,25].

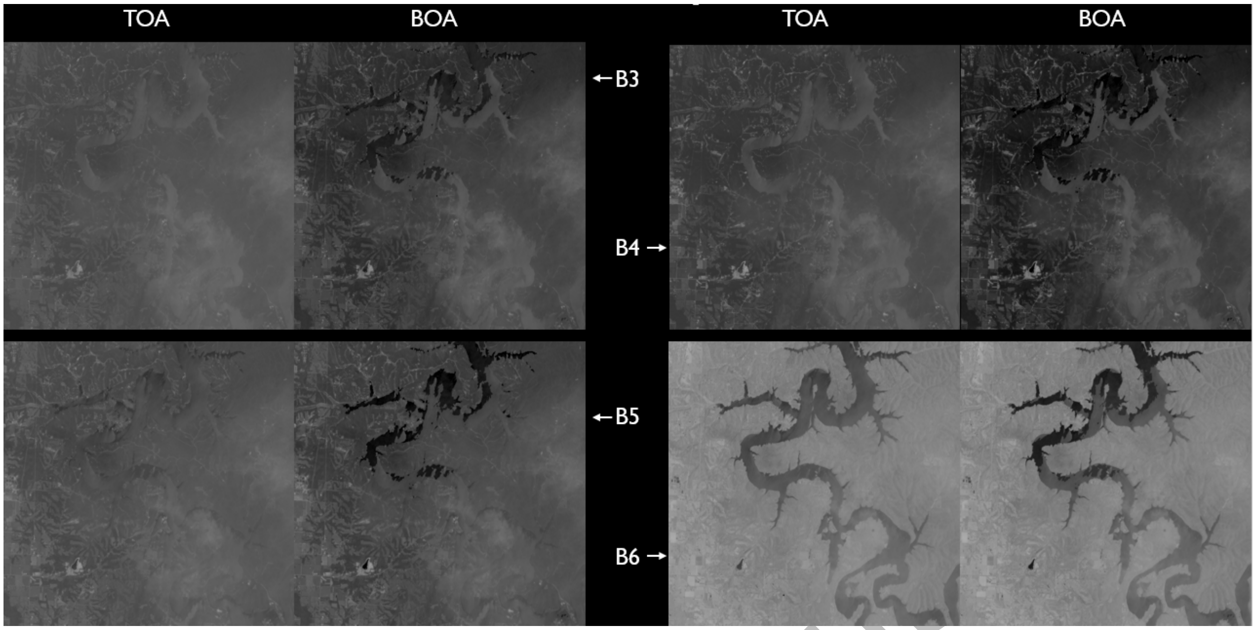

Figure 6 ACOLITE's atmospherically uncorrected TOA and corrected BOA of the Sentinel-2B L1C MSI product for the Southwest portion of the Beaver Lake, Arkansas area on July 11, 2019.

4. Conclusions

An analysis of the results indicates these methods were unsuccessful as implemented and require further improvement. Both the Pearson correlation coefficient and coefficient of determination were outside the bound of statistical significance for both methods of CHL-*a* estimation and for DOC estimation. Only turbidity showed a strong positive correlation with the corresponding B4. Possible sources of error for this assessment include the usage of imagery containing cloud cover, and unavailable in-situ reflectance values for correction purposes. Further investigations into the usage of band ratios to predict lake water quality at Beaver Lake should involve strict selection of entirely cloud-free imagery and the usage of different band ratios from the literature. Less linear band math could be what is necessary for Beaver Lake's unique needs. A further improvement would be collection of in-situ reflectance spectra corresponding to the time of a Sentinel-2 overpass. The spectra would aid the researcher in determining the efficacy of the atmospheric correction by providing known values for BOA.

5. Notes

Note 1 - Due to the way the Copernicus Open Access Hub handles older imagery products, all products retrieved from offline systems must have the <PRODUCT_URI/> line replaced by <PRODUCT_URI>Blank<PRODUCT_URI/> in the MTD_MSIL1C.xml file before used with ACOLITE.

Note 2 - The following parameters were passed to ACOLITE, a geographic region subset of (36.085556,-94.111111,36.427222,-93.709444) and the elevation parameter of 1127 m.

6. Appendix

Band Number	A’s Central Wavelength (µm)	A’s Bandwidth (µm)	B’s Central Wavelength (µm)	B’s Bandwidth (µm)	A&B’s Spatial Resolution (m)
B1	442.7	21	442.3	21	60
B2	492.4	66	492.1	66	10
B3	559.8	36	559.0	36	10
B4	664.6	31	665.0	31	10
B5	704.1	15	703.8	16	20
B6	740.5	15	739.1	15	20
B7	782.8	20	779.7	20	20
B8	832.8	106	833.0	106	10
B8a	864.7	21	864.0	22	20
B9	945.1	20	943.2	21	60
B10	1373.5	31	1376.9	30	60
B11	1613.7	91	1610.4	94	20
B12	2204.4	175	2185.7	185	20

Table 3 Spectral and spatial resolutions of each band on the respective MSI of both Sentinel-2A and Sentinel-2B [20].

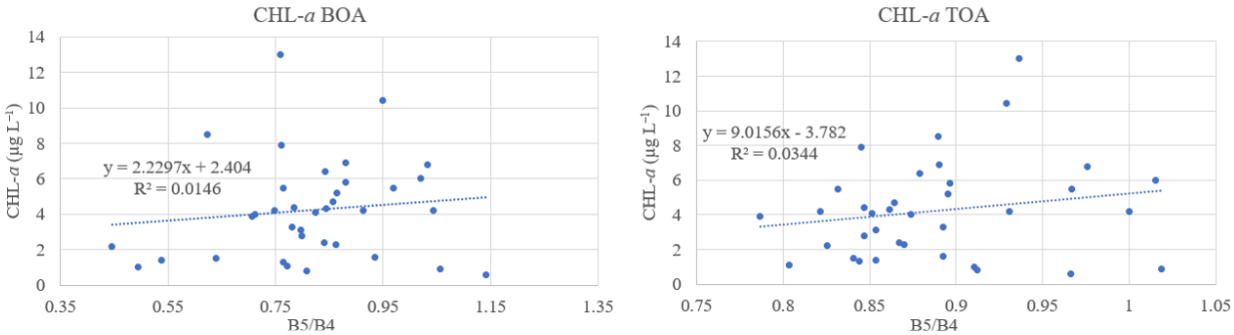

Figure 7 Represents correlation of the B4 reflectance from L1C products to in-situ turbidity data for both the atmospherically corrected BOA reflectance on the left and the uncorrected TOA reflectance on the right.

References

1. Alparslan, E., Coskun, H. G., & Alganci, U. (2009). Water quality determination of Küçükçekmece Lake, Turkey by using multispectral satellite data. *The Scientific World Journal*, *9*, 1215-1229.
2. Ansper, A., & Alikas, K. (2019). Retrieval of Chlorophyll a from Sentinel-2 MSI Data for the European Union Water Framework Directive Reporting Purposes. Remote Sensing, 11(1), 64.
3. Arar, E. J., & Collins, G. B. (1997). Method 445.0: In vitro determination of chlorophyll a and pheophytin a in marine and freshwater algae by fluorescence. Ohio: United States Environmental Protection Agency, Office of Research and Development, National Exposure Research Laboratory.
4. Biehl, L., & Landgrebe, D. (2002). MultiSpec—a tool for multispectral–hyperspectral image data analysis. *Computers & Geosciences*, *28*(10), 1153-1159.

5. Chen, Q., Zhang, Y., & Hallikainen, M. (2007). Water quality monitoring using remote sensing in support of the EU water framework directive (WFD): A case study in the Gulf of Finland. Environmental Monitoring and Assessment, 124(1-3), 157-166.
6. Cox Jr, R. M., Forsythe, R. D., Vaughan, G. E., & Olmsted, L. L. (1998). Assessing water quality in Catawba River reservoirs using Landsat thematic mapper satellite data. *Lake and Reservoir Management*, *14*(4), 405-416.
7. Drusch, M., Del Bello, U., Carlier, S., Colin, O., Fernandez, V., Gascon, F., Hoersch, B., Isola, C., Laberinti, P., Marimort, P., Meygret, A., Spoto, F., Sy., O., Marchese, F., & Bargellini, P. (2012). Sentinel-2: ESA's optical high-resolution mission for GMES operational services. *Remote sensing of Environment*, *120*, 25-36.
8. The Enhanced Thematic Mapper Plus Landsat Science. (n.d.). Retrieved April 1, 2020, from https://landsat.gsfc.nasa.gov/the-enhanced-thematic-mapper-plus/
9. EPA, U. (1993). Method 180.1: Determination of Turbidity by Nephelometry. Rev. 2.0. *Methods for Chemical Analysis of Water and Wastes*.
10. European Space Agency. Copernicus Open Access Hub https://scihub.copernicus.eu/dhus/#/home
11. European Space Agency. *Sentinel-2 User Handbook*; ESA Standard Document; ESA: Paris, France, 2015.
12. Gholizadeh, A., Žižala, D., Saberioon, M., & Borůvka, L. (2018). Soil organic carbon and texture retrieving and mapping using proximal, airborne and Sentinel-2 spectral imaging. *Remote Sensing of Environment*, *218*, 89-103.
13. Gholizadeh, M., Melesse, A., & Reddi, L. (2016). A comprehensive review on water quality parameters estimation using remote sensing techniques. Sensors, 16(8), 1298.
14. Gitelson, A. (1992). The peak near 700 nm on radiance spectra of algae and water: relationships of its magnitude and position with chlorophyll concentration. *International Journal of Remote Sensing*, *13*(17), 3367-3373.
15. Gomarasca, M. A., Giardino, C., Bresciani, M., De Carolis, G., Sandu, C., Tornato, A., Spizzichino, A., Valentini, E., Taramelli, A., & Tonolo, F. G. Italy. (2019). Copernicus Sentinel missions for Water Resources.
16. Japitana, M. V., & Burce, M. E. C. (2019). A Satellite-based Remote Sensing Technique for Surface Water Quality Estimation. *Engineering, Technology & Applied Science Research*, *9*(2), 3965-3970.
17. Kapalanga, T. S. (2015). Assessment and development of remote sensing based algorithms for water quality monitoring in Olushandja Dam, North-Central Namibia.
18. Kontopoulou, E., Kolokoussis, P., & Karantzalos, K. (2017). Water quality estimation in Greek lakes from Landsat 8 multispectral satellite data. *European Water*, *58*, 191-196.
19. Liu, H., Xu, M., & Beck, R. (2018, July). An Ensemble Approach to Retrieving Water Quality Parameters from Multispectral Satellite Imagery. In IGARSS 2018-2018 IEEE International Geoscience and Remote Sensing Symposium (pp. 9284-9287). IEEE.
20. MultiSpectral Instrument (MSI) Overview. (n.d.). Retrieved April 1, 2020, from https://earth.esa.int/web/sentinel/technical-guides/sentinel-2-msi/msi-instrument
21. Papoutsa, C., Retalis, A., Toulios, L., & Hadjimitsis, D. G. (2014). Defining the Landsat TM/ETM+ and CHRIS/PROBA spectral regions in which turbidity can be retrieved in inland waterbodies using field spectroscopy. *International Journal of Remote Sensing*, *35*(5), 1674-1692.

22. Ritchie, J. C., Zimba, P. V., & Everitt, J. H. (2003). Remote sensing techniques to assess water quality. Photogrammetric Engineering & Remote Sensing, 69(6), 695-704.
23. Shafique, N. A., Fulk, F., Autrey, B. C., & Flotemersch, J. (2003, October). Hyperspectral remote sensing of water quality parameters for large rivers in the Ohio River basin. In *First interagency conference on research in the watershed, Benson, AZ* (pp. 216-221).
24. Sudheer, K. P., Chaubey, I., & Garg, V. (2006). Lake water quality assessment from landsat thematic mapper data using neural network: an approach to optimal band combination selection1. *JAWRA Journal of the American Water Resources Association*, *42*(6), 1683-1695.
25. Sriwongsitanon, N., Surakit, K., & Thianpopirug, S. (2011). Influence of atmospheric correction and number of sampling points on the accuracy of water clarity assessment using remote sensing application. *Journal of Hydrology*, *401*(3-4), 203-220.
26. Toming, K., Kutser, T., Laas, A., Sepp, M., Paavel, B., & Nõges, T. (2016). First experiences in mapping lake water quality parameters with Sentinel-2 MSI imagery. Remote Sensing, 8(8), 640.
27. Vanhellemont, Q. (2019). Adaptation of the dark spectrum fitting atmospheric correction for aquatic applications of the Landsat and Sentinel-2 archives. *Remote Sensing of Environment*, *225*, 175-192.
28. Vanhellemont, Q., & Ruddick, K. (2016, May). Acolite for Sentinel-2: Aquatic applications of MSI imagery. In *Proceedings of the 2016 ESA Living Planet Symposium, Prague, Czech Republic* (pp. 9-13).
29. Vanhellemont, Q., & Ruddick, K. (2018). Atmospheric correction of metre-scale optical satellite data for inland and coastal water applications. *Remote Sensing of Environment*, *216*, 586-597.
30. The Water Quality Portal. https://www.waterqualitydata.us/portal/
31. Watershed Maps: Beaver Lake. (2016, December 1). Retrieved April 1, 2020, from https://www.bwdh2o.org/beaver-lake/watershed-maps/
32. Williams, T., Foreman, W. T., Decess, J., Reed-Parker, C., & Stevenson, D. L. (2015). National Water Quality Laboratory technical memorandum 15.02—Changes to National Water Quality Laboratory (NWQL) procedures used to establish and verify laboratory detection and reporting limits. *US Geological Survey*.
33. Zhu, W., Yu, Q., Tian, Y. Q., Becker, B. L., Zheng, T., & Carrick, H. J. (2014). An assessment of remote sensing algorithms for colored dissolved organic matter in complex freshwater environments. *Remote Sensing of Environment*, *140*, 766-778.